The Amorphous Phase in High-Speed Spun PET Fibers

K. L. PENG* and C. M. ROLAND

Chemistry Division, Code 6120, Naval Research Laboratory, Washington, DC 20375-5000

SYNOPSIS

Two phenomenogical descriptions of oriented semicrystalline polymers, the series-parallel model and the series-aggregate model, were applied to poly(ethylene terephthalate) (PET) fibers obtained at different spinning speeds. The mechanical behavior of the fibers conformed well to both models. The analyses indicate that PET fibers obtained by high-speed spinning possess a more compliant interfibrillar amorphous phase. This feature may account for both the greater dimensional stability, as well as the more reversible mechanical behavior, exhibited by high-speed spun PET. © 1993 John Wiley & Sons, Inc.

Keywords: poly(ethylene terephthalate) • series-parallel model • series-aggregate model • high-speed spinning

INTRODUCTION

Poly(ethylene terephthalate) is commercially the most important polyester, and hence much effort is expended toward improving the physical properties of PET-based materials. A variety of approaches have been explored to increase the stiffness, strength, and dimensional stability of PET fibers, including controlled drawing[1-5] and the related zone annealing,[6-9] incremental drawing,[10] high-pressure crystallization,[11,12] high-pressure extrusion,[13-16] and high-temperature crystallization.[17] High-speed spinning (HSS) is a processing innovation that has made a significant impact. At sufficiently high spinning (or wind-up) speeds, whereby the birefringence of the yarn attains a value of 0.06 or higher, markedly higher density and melting temperatures result, indicating the development of crystallization in the spin line.[18-23] Higher spinning speed results in higher extension of the PET molecules.[18,22,24,25] The oriented chain segments act as nucleation sites for crystallization, accelerating the rate of crystallization[18,24,25] with a less oriented amorphous phase resulting.[19,25-27] The particular spinning speed associated with the onset of crystallization in the spin line depends on the molecular weight of the PET.

The properties of PET yarn as spun can be plausibly related to the HSS processing conditions.[20,26-29] However, evidently there are structural changes effected by the spinning that are only manifested when the yarn is subsequently drawn. For example, while the dimensional stability (i.e., length change upon heating beyond T_g) of the as-spun yarn is expected to parallel the amorphous orientation, HSS fibers after drawing are reputed to exhibit higher dimensional stability than conventional PET fibers.[28-30] For undrawn yarn, the shape of the stress–strain curve is independent of spinning speed[27]; conversely, the stress–strain behavior of HSS fibers after drawing markedly differs from that of conventional PET fibers.[28-30] Similarly, the breaking stress measured for as-spun PET is independent of spinning speed, while the strength of drawn PET varies inversely with spinning speed.[20,26] To account for the modulus of a conventional fiber, consideration of only the degree of crystallinity and the amorphous phase orientation may suffice[26,31,32]; on the other hand, the amorphous orientation of drawn HSS fibers with comparable degrees of crystallinity does not correlate with either their modulus or shrinkage.[28,29] All these results reveal that some structural features that arise during HSS persist and only become evident through subsequent drawing.

It is not obvious how spin-line crystallization per

* Present affiliation: Polymer Technology Group, Bausch & Lomb, Boston, MA.

Journal of Polymer Science: Part B: Polymer Physics, Vol. 31, 1339–1345 (1993)
 CCC 0887-6266/93/101339-07

se might be responsible for the distinctive behavior of drawn HSS PET. Although these fibers are recognized as offering performance advantages,[29,30] an understanding of their morphology is currently lacking. Full exploitation of the high-speed spinning process may only be realized when the detailed relationships between structure, properties, and processing have been established. The present work attempts to characterize the mechanical behavior of drawn PET yarns, spun both at conventional and at high speed. These results are intended to facilitate development of a realistic model to describe the defining structural features of drawn HSS PET fibers.

EXPERIMENTAL

The 1000 denier (0.08 mm^2 cross-sectional area) PET fibers were obtained from the Industrial Fibers Division of Allied-Signal Corp. Sample designations are given in Table I of the preceding paper.[31] The yarns were spun at increasing take-up speeds ranging from conventional spinning to the range associated with spin-line crystallization. The fibers were subsequently drawn to near their maximum draw ratio, followed by conventional heat treatment. The morphologies and mechanical properties of the undrawn yarns, along with some treated cord results, have been reported previously.[28-31]

Shrink-force measurements were carried out with a Rheovibron instrument on which the dynamic mechanical facility was inoperative. The static stress was measured at a fixed specimen length as the temperature was scanned 2°/min. For this experiment, the fiber denier was reduced (typically by about 60%) to eliminate instrumental compliance errors.

Tensile testing was done with an Instron 4206 instrument at room temperature using a cross-head speed of 10 mm/min. To avoid end effect errors, the initial sample length was typically 580 mm, with the specimen clamped by a jig on which the fiber ends were wrapped several times.

Combined static and dynamic experiments were done on an Imass Corp. Dynastat Mark II mechanical spectrometer. The static and dynamic stresses were 135 and 6 MPa, respectively. The (constant) creep stress was below the level at which irreversible behavior (described below) arises. A frequency of 90 Hz was used to facilitate separation of the static and dynamic components of the response.

RESULTS

Shrinkage Stress

The temperature dependence of the stress for fibers held at fixed length is shown in Figure 1. This stress depends directly on the molecular extension, but only develops a measurable magnitude at temperatures beyond the glass transition temperature of PET (ca. 80°C). At sufficiently high temperatures (> 115°C), enhanced chain mobility permits crystallization to occur over the time scale of the experiment, with a concomitant reduction in stress. Between these extremes of the glass transition and thermal crystallization, the retractive stress is directly proportional to temperature, consistent with its entropic origin.

It is tempting to interpret the mechanical response of the fibers in terms of the number and orientation of elastically active chains.[33-35] However, while the stress depends directly on the number of oriented chains, the dependence of the retractive stress on macroscopic strain is uncertain (constituting the focus of rubber elasticity theories). The temperature derivative of the elastic stress $(\partial\sigma/\partial T)_L$ (given in Table I) for each fiber can be compared to the amorphous orientation. Both the elastic stress of a flexible chain polymer and the Hermans orientation function f_a for the amorphous phase are directly proportional to the second moment of the orientation function of the chain segments.[36,37] The amorphous orientation has been previously reported

Table I. Mechanical Results

Fiber	$(\partial\sigma/\partial T)$ (GPa deg^{-1})	$f_a/(1 - X_{cr})$ (GPa)	E_{fib}[a] (GPa)	E_a^{intra} (GPa)	E_a^{inter} (GPa)	G_{agg} (GPa)
1W70	0.63	1.06	18.3	10.6	13.3	1.45
1W90	0.54	0.91	15.6	7.5	12.8	0.75
A330	0.45	0.89	16.7	11.0	10.6	0.76
EXP	0.43	0.77	15.3	11.7	8.2	0.60

[a] Dynamic at 90 Hz.

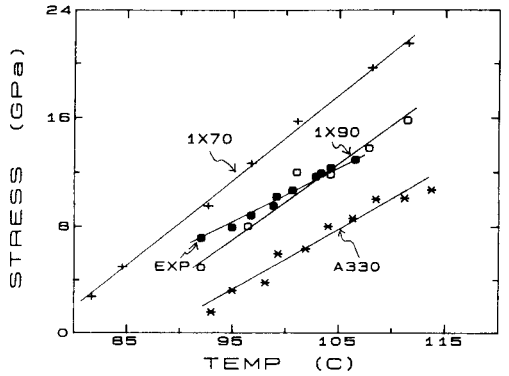

Figure 1. Retractive stress measured at temperatures between the glass transition temperature and the crystallization temperature of PET. Fibers were held at fixed length during the measurement. Intercepts for the data reflect the initial (nearly zero) tension.

for these fibers.[28,29] For simple series coupling of the crystalline and amorphous domains, whereby the stress is equal for the two phases,[32,38] the fiber modulus depends only on the concentration and modulus of the amorphous phase. The modulus of the amorphous chains is governed primarily by their degree of orientation, so that in this situation the fiber modulus can be accounted for solely in terms of f_a and the degree of crystallinity X_{cr} of the PET. Indeed, it has been reported that the shrinkage of HSS PET correlates uniquely with the quantity $(1 - X_{cr})f_a$, congruent with a homogeneous stress condition.[26] Since crystallization and amorphous-phase orientation both effect the *gauche* to *trans* conformational transition in PET, there is an excellent correlation between the modulus of conventional PET fibers and the concentration of *trans* rotamers.[32] Thus, for a uniform stress condition (i.e., negligible interfibrillar amorphous material) in which the crystalline phase is much stiffer than the amorphous material, the following relation is expected to hold:

$$E_{fib} \propto \left(\frac{\partial \sigma}{\partial T}\right)_L \propto \frac{f_a}{1 - X_{cr}} \qquad (1)$$

The temperature dependence of the retractive stress (from Figure 1) is listed in Table I for each fiber together with the quantity on the right-hand side of eq. (1). The predicted correlation is weak at best, demonstrating the limitations of a description of the fiber morphology predicated upon a homogeneous-stress condition.

The inadequacy of the two-phase model for the fibers studied herein is corroborated by various other experimental observations. The X-ray scattering results described in the preceding article[31] are in contradiction to the homogeneous stress distribution implicit in a series coupling of the phases. Solid-state NMR measurements on these fibers yield direct evidence for the existence of three phases, distinguishable by the mobility of their constituent chains.[39] It is interesting to note that even in unoriented semicrystalline PET obtained by isotropic crystallization, small-angle X-ray scattering measurements suggested the existence of two different amorphous components.[41]

Series-Parallel Model

Several three-phase models have been proposed for oriented PET.[41-43] In a model specifically addressing HSS fibers, the amorphous phase is comprised of highly oriented and interconnected noncrystalline chains interspersed among unoriented amorphous polymer domains.[25] An obvious approach for highly drawn flexible chain polymers is the series-parallel model,[44-46] whereby an amorphous phase exists both in series (intrafibrillar chains) and in parallel (interfibrillar chains) to the crystallites. On the assumption that the intrafibrillar and interfibrillar amorphous phases have the same modulus, the series-parallel model gives for the fiber modulus[45]

$$E_{fib} = (1 - X_\perp)E_a + \frac{X_\perp}{X_\parallel/E_{cr} + (1 - X_\parallel)/E_a} \qquad (2)$$

where the product of the longitudinal $X_\parallel$ and the transverse $X_\perp$ degrees of crystallinity yields the total crystallinity. From knowledge of the fiber modulus, along with values for X_{cr}, $X_\parallel$, and inferentially $X_\perp$, values for the amorphous phase modulus, E_a, of PET fibers can be deduced. However, it is unrealistic to expect that amorphous chains within and between the fibrils should have identical mechanical behavior. Various descriptions of fiber morphology[46,47] attribute different degrees of orientation to intrafibrillar and interfibrillar amorphous chains. Crystallization of PET yarn at constant length, which changes only the transverse dimensions of the crystallites, is one example of a process that must alter the interfibrillar chains without effecting a concomitant alteration of the intrafibrillar amorphous phase.

The modulus of the two types of amorphous chains must be distinguished in order to describe accurately the mechanical behavior of the fiber. The X-ray modulus (that is, the crystal lattice strain divided by the macroscopic fiber stress) determined

for these fibers[31] provides a direct measure of the stress on the crystallites. For the series-parallel model the X-ray modulus (or apparent crystal modulus) is given by[44]

$$E_{\text{X-ray}} = X_{\perp}E_{\text{cr}} + (1 - X_{\perp})X_{\parallel}E_a^{\text{inter}} + (1 - X_{\perp})(1 - X_{\parallel})E_{\text{cr}}\frac{E_a^{\text{inter}}}{E_a^{\text{intra}}} \quad (3)$$

where for PET the crystal modulus E_{cr} = 110 GPa.[31,44] This expression allows assessment of the magnitude of E_a^{inter} and E_a^{intra}, representing respectively the interfibrillar and intrafibrillar amorphous moduli (corresponding to chains mechanically coupled in parallel or in series with the crystalline domains). The moduli refer in all cases to deformations parallel to the fiber.

From the low-strain elastic moduli measured herein (Table I) and the crystallinities determined from small-angle and wide-angle X-ray measurements,[31] values for E_a^{inter} and E_a^{intra} can be determined that are consistent with eq. (3). These results are given in Table I. Of greatest interest here, the conventionally spun 1W70 has a higher interfibrillar modulus than do any of the HSS fibers.

Series-Aggregate Model

The approach employed above, in which the fiber properties are regarded as consequences of both the properties of the individual phases and the manner in which they are mechanically coupled to one another, is intuitively appealing. An alternative is the series-aggregate model, which does not explicitly consider the amorphous phase, but provides a phenomenological description of the mechanical behavior of oriented polymers.[48-51] The fiber is viewed as a collection of crystallites (the "aggregates") mechanically coupled in series to one another. The application of tensile stress causes extension of the aggregates and their rotation into alignment with the stretching direction. The latter mechanism is viewed as a shear deformation governed by the "interfibrillar shear modulus" of the fibrils. In this model the influence of the amorphous phase is indirect, since there is no specific consideration of any phase with elastic properties different from those of the crystallites.[52] While the model has been shown to provide a good description of the properties of rigid-rod polymers, such as poly(*p*-phenylene terephthalamide),[50-52] the neglect of any contribution to the mechanical properties from a discrete amorphous phase is implausible for flexible-chain polymers. Surprisingly, however, the model apparently succeeds when applied to polymers such as cellulose[53] and PET.[54]

In the series-aggregate model, the strain and rotation of the aggregates in response to uniaxial stress govern the mechanical response of the fiber.[50,51] The tensile modulus of the aggregates is identified with the crystal modulus, with the fiber compliance being given by[50,51]

$$S_{\text{fib}} = \frac{1}{E_{\text{cr}}} + \frac{\langle \sin^2\phi \rangle}{2G_{\text{agg}}} \quad (4)$$

where G_{agg} is the shear modulus for deformation parallel to the fiber and ϕ is the angle the latter makes with the aggregates. For a well-oriented fiber, it is assumed that creep is caused by rotation of the aggregates with no structural changes occurring. Hence, G_{agg} is constant, and the decrease in the dynamic compliance during creep is attributed solely to orientation of the aggregates. In this case, the creep strain ϵ of the fiber changes with time according to[54]

$$\frac{d\epsilon}{dt} = -G_{\text{agg}}\frac{dS_{\text{fib}}}{dt} \quad (5)$$

The model thus predicts a direct proportionality during creep between the strain and the dynamic compliance of the fiber. The proportionality constant is the phenomenological interfibrillar shear modulus.

Creep and dynamic mechanical measurements were simultaneously obtained on the PET fibers. As seen in Fig. 2, the results confirm the prediction of a proportionality between the time dependencies of ϵ and S_{fib}, indicating some applicability of the model

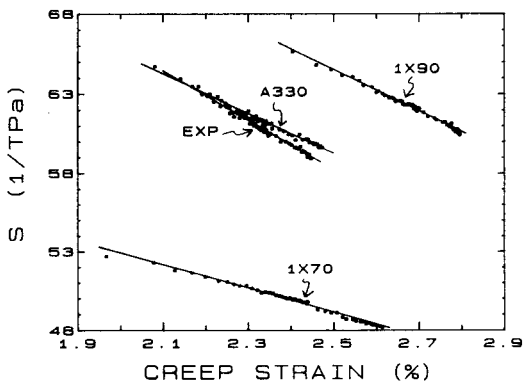

Figure 2. Dynamic compliance measured during creep of fibers (T = 30°C).

to the PET fibers. The values for G_{agg} obtained from the slopes in Figure 2 are listed in Table I. High-speed spinning is associated with a lower G_{agg} in the drawn fiber than for conventional spinning speeds. This result is consistent with, and may in fact directly reflect, the relative magnitudes of E_a^{inter} determined for the fibers using the series-parallel model.

Tensile Stress at Intermediate Extensions

The preceding measurements have been limited to low strains, but in general the mechanical response of the fibers is nonlinear. Even the relative magnitude of the fibers' moduli is altered when comparisons are made at different strains. For example, at intermediate extensions the HSS fibers exhibit a higher modulus than 1W70, while the situation is reversed at strains lower than about 1% elongation.[28,29]

To examine this strain dependence, the fibers were stretched to 2.5% extension and retracted, after which the elongation was repeated (Figure 3). During the second extension cycle, 1W90 exhibits a higher modulus even at very low strains, primarily because the modulus of 1W70 has been significantly reduced by straining. The hysteresis (the fraction of the input strain energy lost during cyclical straining) increases with the magnitude of the reversal strain for 1W70. For 1W90, as well as the other HSS fibers, this quantity is essentially constant with respect to reversal strain. The changes effected by the initial extension were observed to persist without recovery. Evidently the higher modulus at low strain initially measured for 1W70 is due to contributions to its stress that are irreversibly lost upon deformation to strains beyond about 1%.

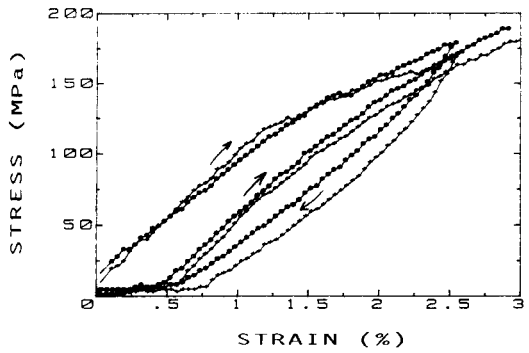

Figure 3. Reversing stress–strain curves for 1W70 (+++) and 1W90 (OOO). The arrows indicate the direction of cross-head travel. The accuracy of the data below about 0.2% strain is uncertain owing to cross-head inertia and sample loading.

DISCUSSION AND SUMMARY

A principle finding is that drawn PET fibers obtained by high-speed spinning possess a more compliant interfibrillar amorphous phase. This conclusion is arrived at indirectly by two different approaches: the series-parallel model, which explicitly considers interfibrillar and intrafibrillar amorphous phases, and the series-aggregate model, in which the contribution of the amorphous chains to the fiber properties is embodied in a phenomenological "interfibrillar shear modulus." Although the latter physical description of the PET morphology is unrealistic, the conformity of the experimental results in Figure 2 to the series-parallel model suggest that the inferences concerning fiber morphology may be valid.

In the preceding paper[31] the morphology transverse to the fibrils was deduced from X-ray scattering experiments (see Fig. 5 in ref. 31). For the HSS fibers, the decreasing E_a^{inter} and G_{agg} inferred herein are compatible with the apparent reduction of the interfacial area of the fibrils in the transverse direction.[31]

Although the intrafibrillar amorphous phase may contribute to a fiber's dimensional stability, the interfibrillar tie molecules will dominate the measured fiber shrinkage behavior if they are significantly longer. An increasing extent of spin-line crystallization selectively removes the more oriented amorphous chains (through their conversion to the crystalline phase).[18-27] This is probably the origin of the high compliance of the interfibrillar amorphous phase in the HSS fibers, which is consistent with their greater dimensional stability.[28,29]

The fiber modulus itself is also lower for the HSS fibers, but this cannot be accounted for simply by their lower amorphous orientation, nor in terms of some combination of f_a and their degree of crystallinity. An earlier suggestion[26] that differences in shrinkage and modulus between conventional and HSS PET fibers reflect differences in their degrees of crystallinity is not relevant here. Although the fiber modulus is not a unique function of either G_{agg} or of E_a, certainly the compliance of the interfibrillar amorphous phase of the HSS fibers contributes to their lower modulus. Other subtle differences in supermolecular structure evidently exist; however, such details are not revealed easily.

One hypothesis is that the high-speed spinning

process produces a less back-folded crystalline structure.[18] The crystalline phase in HSS PET would then consist of a carcass of extended chain crystals, formed during orientational crystallization in the spin line, along with a folded-chain crystal overgrowth. Extended-chain crystallization of PET has been achieved by different processing methods.[5,17] The presence of this form of crystal connectivity would affect the fiber modulus in a manner unaccounted for by consideration only of the amorphous phase. The crystal connectivity associated with an extended-chain structure would contribute to higher modulus and lower shrinkage, but the low $E_{\text{X-ray}}$ measured for these fibers[31] argues against any significant extended-chain crystallinity.

The irreversibility of the 1W70 response to strains beyond about 1% is due to some morphological changes, perhaps fracture of the more taut chains within the amorphous phase. These interconnecting strands represent the high end of the amorphous-phase orientation distribution corresponding to a measured f_a. Such mechanical irreversibility is unobserved in the HSS fibers, in accord with their lower E_a^{inter}. The higher modulus of the HSS fibers at intermediate strains (> 1%) arises from an absence of chain scission during straining, due to fewer taut tie-chains in the interfibrillar regions of the HSS fibers. This intermediate strain behavior is very significant for applications of PET fibers.[28-30]

This work was supported by the Allied-Signal Corporation and the Office of Naval Research. The authors express their appreciation to Dr. C. J. Nelson, Dr. P. B. Rim, and Mr. C. A. Trask for stimulating discussions and helpful suggestions.

REFERENCES AND NOTES

1. S. Fakirov and M. Evstatiev, *Polymer,* **31,** 431 (1990).
2. A. Misra and R. S. Stein, *J. Polym. Sci., Polym. Phys. Ed.,* **17,** 235 (1979).
3. M. Matsuo, M. Tamada, T. Teradam, C. Sawatari, and M. Niwa, *Macromolecules,* **15,** 988 (1982).
4. V. V. Krenev, M. I. Simonova, E. M. Aizenshtein, V. G. Baranov, and S. Y. Frenkel, *Fiber Chem.,* **1,** 53 (1978).
5. C. M. Roland and M. F. Sonnenschein, *Polym. Eng. Sci.,* **31,** 1434 (1991).
6. T. Kunugi, A. Suzuki, and M. Hashimoto, *J. Appl. Polym. Sci.,* **26,** 213 (1981).
7. T. Kunugi, C. Ichinose, and A. Suzuki, *J. Appl. Polym. Sci.,* **31,** 429 (1986).
8. G. Hinrichsen, P. Wolbring, and H. Springer, in *Interrelations Between Processing, Structure and Properties of Polymeric Materials,* J. C. Seferis and P. S. Theocaris (eds.), Elsevier, Amsterdam, 1984.
9. D. Hofmann, U. Goschel, E. Walenta, D. Geiss, and B. Philipp, *Polymer,* **30,** 242 (1989).
10. M. V. Sussman, *Fiber World* April (1985) 58.
11. A. Siegmann and P. J. Harget, *J. Polym. Sci., Poly. Phys. Ed.,* **18,** 2181 (1980).
12. P. J. Phillips and H. T. Tseng, *Macromolecules,* **22,** 1649 (1989).
13. P. D. Griswold and J. A. Cuculo, *J. Appl. Polym. Sci.,* **22,** 163 (1978).
14. J. R. C. Pereira and R. S. Porter, *J. Polym. Sci., Polym. Phys. Ed.,* **21,** 1133 (1983).
15. T. Sun, A. Zhang, F. M. Li, and R. S. Porter, *Polymer,* **29,** 2115 (1988).
16. A. E. Zachariades and R. S. Porter, in *The Strength and Stiffness of Polymers,* A. E. Zachariades and R. S. Porter (eds.), Marcel Dekker, New York, 1983.
17. C. M. Roland, *Poly. Eng. Sci.,* **31,** 849 (1991).
18. H. M. Heuvel and R. Huisman, *J. Appl. Poly. Sci.,* **22,** 2229 (1978).
19. H. H. George, A. Holt, and A. Buckley, *Polym. Eng. Sci.,* **23,** 95 (1983).

19a. Shimizu

20. H. Brody, *J. Macromol. Sci. Phys.,* **B22,** 407 (1983).
21. A. Ziabicki and L. Jarecki, in *High-Speed Fiber Spinning,* A. Ziabicki and H. Kawai (Eds.), Wiley, New York, 1985.
22. S. K. Garg, *J. Appl. Polym. Sci.,* **29,** 2111 (1984).
23. J. M. Schultz, *Polym. Sci. Eng.,* **31,** 661 (1991).
24. P. Desai and A. S. Abhiraman, *J. Polym. Sci., Poly. Phys. Ed.,* **26,** 1657 (1988).
25. H. A. Hristov and J. M. Schultz, *J. Polym. Sci., Poly. Phys. Ed.,* **28,** 1647 (1990).
26. R. Huisman and H. M. Heuvel, *J. Appl. Polym. Sci.,* **37,** 595 (1989).
27. G. Perez in *High Speed Fiber Spinning: Science and Engineering Aspects,* A. Ziabicki and H. Kawai, (eds.), Wiley, New York, 1985.
28. P. B. Rim and C. J. Nelson, *J. Appl. Poly. Sci.,* **42,** 1807 (1991).
29. P. B. Rim and C. J. Nelson, *Rubber World,* **204,** 30, (1991).
30. P. B. Rim and C. J. Nelson, *J. Texas Inst.,* **83,** 78 (1992).
31. D. Tomlin, C. M. Roland, and L. A. Slutsker, *J. Polym. Sci., Polym. Phys. Ed.,* **31,** 1331 (1993).
32. S. R. Padibjo and I. M. Ward, *Polymer,* **24,** 1103 (1983).
33. A. Cunningham, I. M. Ward, H. A. Willis, and V. Zichy, *Polymer,* **15,** 749 (1974).
34. J. Purvis and D. I. Bower, *J. Polym. Sci., Polym. Phys. Ed.,* **14,** 1461 (1976).
35. S. D. Long and I. M. Ward, *J. Appl. Polym. Sci.,* **42,** 1921 (1991).
36. Y. Shindo and R. S. Stein, *J. Polym. Sci. A-2,* **7,** 2115 (1969).
37. L. R. G. Treloar, *Rep. Prog. Phys.,* **36,** 755 (1973).

38. K. Nakamae, T. Nishino, F. Yokoyama, and T. Matsumoto, *J. Macromol. Sci.-Phys.*, **B27,** 407 (1988).
39. J. H. Walton, J. B. Miller, and C. M. Roland, to be published.
40. Santa Cruz, N. Stribeck, H. G. Zachmann, and F. J. Balta Calleja, *Macromolecules,* **24,** 5980 (1991).
41. J. R. Havens and D. L. VanderHart, *Macromolecules,* **18,** 1663 (1985).
42. E. W. Fischer and S. Fakirov, *J. Mat. Sci.,* **11,** 1041 (1976).
43. A. Peterlin, in *Ultra High Modulus Polymers* A. Ciferri and I. M. Ward (eds.), Applied Science, London, 1979.
44. T. Thistlewaite, R. Jakeways, and I. M. Ward, *Polymer,* **29,** 61 (1988).
45. D. C. Prevorsek, P. J. Harget, R. K. Sharma, and A. C. Reimschuessel, *J. Macromol. Sci. B,* **8,** 127 (1973).
46. D. C. Prevorsek, G. A. Tirpak, P. J. Harget, and A. C. Reimschuessel, *J. Macromol. Sci. B,* **9,** 733 (1974).
47. A. Peterlin, *Polym. Eng. Sci.,* **19,** 118 (1979).
48. S. M. Crawford and H. Kolsky, *Proc. Phys. Soc.,* **B64,** 119 (1951).
49. I. M. Ward, *Mechanical Properties of Solid Polymers,* John Wiley, New York, 1983.
50. M. G. Northolt, *Polymer,* **21,** 1199 (1980).
51. M. G. Northolt and R. van der Hout, *Polymer,* **26,** 310 (1985).
52. M. G. Northolt and J. J. van Aartsen, *J. Polym. Sci. Poly. Symp.,* **58,** 283 (1977).
53. M. G. Northolt and H. de Vries, *Die Ange. Makro. Chem.,* **133,** 183 (1985).
54. M. G. Northolt, A. Roos, and J. H. Kampschreur, *J. Polym. Sci., Polym. Phys. Ed.,* **27,** 1107 (1989).

Received June 1, 1992
Accepted December 30, 1992